

Formation of Hydride, Formyl, Hydroxymethyl, Dimetal Ketone, and Ethylene-Bridged Species from Small-Molecule Substrate Reactions with Rhodium Complexes of an N₄ Nonmacrocylic Ligand

Mingli Wei and Bradford B. Wayland*

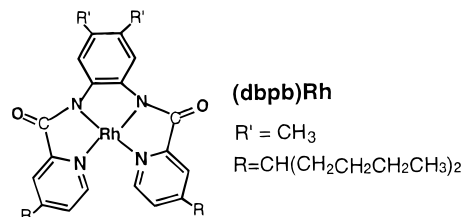
Department of Chemistry, University of Pennsylvania, Philadelphia, Pennsylvania 19104-6323

Received June 18, 1996[®]

Summary: Reactions of the rhodium(II) dimer [(dbpb)-Rh]₂ (**1**) ((dbpb)H₂ (**2**) = 4,5-dimethyl-1,2-bis((4-(1-butylpentyl))pyridine-2-carboxamido)benzene) with H₂, CO, and CH₂=CH₂ produce a rhodium(III) hydride, (dbpb)Rh-H (**3**), dirhodium ketone, (dbpb)Rh-C(O)-Rh(dbpb) (**4**), and an ethylene-bridged complex, (dbpb)-Rh-CH₂CH₂-Rh(dbpb) (**5**), respectively. The rhodium(III) hydride (**3**) reacts with CO and H₂CO to produce formyl, (dbpb)Rh-CHO (**6**), and hydroxymethyl, (dbpb)-Rh-CH₂OH (**7**) complexes. Equilibrium thermodynamic studies for reactions of **1** with hydrogen and ethene and the observed substrate reactions of **1** and **3** indicate that the (dbpb)Rh-H and (dbpb)Rh-C bond dissociation enthalpies are comparable to those for rhodium porphyrin complexes.

Rhodium(II) porphyrins are unusual in having favorable thermodynamic properties for producing metalloformyl complexes from reaction with H₂ and CO¹ and a wide range of other substrate reactions² including methane activation.³ One of the continuing central objectives in this area is to extend the rhodium porphyrin chemistry to complexes with nonmacrocylic ligand systems^{4,5} which have the potential to manifest more versatile reaction pathways and thus faster substrate reactions than those observed for rigid tetradentate macrocylic complexes. Recently reported studies of rhodium salen derivatives by the Eisenberg group⁵ and ourselves⁴ were the initial efforts directed toward this goal. This article reports on reactivity patterns of an N₄ tetradentate nonmacrocylic rhodium(II) dimer,

[(dbpb)Rh]₂ (**1**) ((dbpb)H₂ (**2**)^{6a} = 4,5-dimethyl-1,2-bis((4-(1-butylpentyl))pyridine-2-carboxamido)benzene) with H₂, CO, and CH₂=CH₂ and reactions of the corresponding rhodium hydride with CO and H₂CO.



Reaction of the free ligand (dbpb)H₂ (**2**)^{6a} with rhodium trichloride RhCl₃·xH₂O in refluxing DMF (1 h) produces (dbpb)Rh-Cl, which is subsequently converted to (dbpb)Rh-CH₃.^{6b} Photolysis of the methyl derivative (λ > 350nm) in benzene produces the rhodium(II) dimer, [(dbpb)Rh]₂ (**1**).⁷ Both benzene and THF solutions of [(dbpb)Rh]₂ display narrow ¹H NMR spectra in the temperature range (295–393 K) where (octaethylporphyrinato)rhodium(II) dimer, [(OEP)Rh]₂, manifests substantial exchange broadening from dissociation into paramagnetic monomers,⁸ which is a qualitative indication that **1** has a larger Rh–Rh bond dissociation enthalpy than [(OEP)Rh]₂.

[(dbpb)Rh]₂ (**1**) reacts slowly with hydrogen (P_{H₂} = 0.5 atm, 343 K; 120 h) to produce an equilibrium of **1** and a monomeric metallo hydride complex, (dbpb)Rh-H

(6) (a) The free ligand, (dbpb)H₂, was synthesized by condensation of 4,5-dimethyl-1,2-phenylenediamine and 4-(1-butylpentyl)pyridine-2-carboxylic acid in pyridine in the presence of triphenyl phosphite by literature methods: Barnes, D. J.; Chapman, R. L.; Vagg, R. S.; Watton, E. C. *J. Chem. Eng. Data* **1978**, *23*, 349. Caddy, D. E.; Utley, J. H. *J. Chem. Soc., Perkin 2* **1973**, 1258. ¹H NMR of (dbpb)H₂ (**2**) (C₆D₆, δ): 10.55 (s, 2H, N-H); 8.44 (d, 2H, py, ⁴J = 1.5 Hz); 8.26 (d, 2H, py, ³J = 5.0 Hz); 7.69 (s, 2H, phenyl); 6.73 (d of d, 2H, py, ³J = 5.0 Hz, ⁴J = 1.5 Hz); 2.27 (m, 2H, -CH-); 1.96 (s, 6H, CH₃); 0.7–1.5 (m, 36H, -(CH₂)₃CH₃). LR FAB MS (*m/e*): calc, 598.4; obs, 599. (b) (dbpb)Rh-Cl and (dbpb)Rh-CH₃ were synthesized by published procedures: Mak, S. T.; Yam, V. W.; Che, C. M. *J. Chem. Soc., Dalton Trans.* **1990**, 2555. ¹H NMR of (dbpb)Rh-Cl (**2**) (CD₃CN, δ): 8.92 (d, 2H, py, ³J = 5.6 Hz); 8.48 (s, 2H, phenyl); 7.81 (d, 2H, py, ⁴J = 1.8 Hz); 7.44 (d of d, 2H, py, ³J = 5.6 Hz, ⁴J = 1.8 Hz); 2.73 (m, 2H, -CH-); 2.22 (s, 6H, CH₃); 0.8–2.0 (m, 36H, -(CH₂)₃CH₃). LR FAB MS (*m/e*): calc, 734.3; obs, 734. ¹H NMR of (dbpb)Rh-CH₃ (C₆D₆, δ): 8.64 (s, 2H, phenyl); 8.11 (s, 4H, py); 7.74 (d, 2H, py, ³J = 5.4 Hz); 6.79 (d, 2H, py, ³J = 5.4 Hz); 2.43 (m, 2H, -CH-); 2.19 (s, 6H, CH₃); 1.26 (d, Rh-CH₃, ²J_{Rh-H} = 2.4 Hz); 0.7–1.6 (m, 36H, -(CH₂)₃CH₃). FAB MS (*m/e*): calc, 715.3458; obs, 715.3452.

(7) Photolysis of (dbpb)Rh-CH₃ in dry benzene (λ > 350nm) produces [(dbpb)Rh]₂ (**1**). ¹H NMR (THF, δ): 8.27 (s, 4H, phenyl); 8.08 (d, 4H, py, ³J = 5.2 Hz); 7.37 (s, 4H, py); 6.98 (d, 4H, py, ³J = 5.2 Hz); 2.57 (m, 4H, -CH-); 2.28 (s, 12H, CH₃); 0.8–1.8 (m, 72H, -(CH₂)₃-CH₃). ¹H NMR (C₆H₆, δ) 8.89 (s, 4H, phenyl); 7.97 (d, 4H, py, ³J = 5.4 Hz); 7.85 (s, 4H, py); 6.89 (d, 4H, py, ³J = 5.4 Hz); 2.47 (m, 4H, -CH-); 2.18 (s, 12H, CH₃); 0.8–1.6 (m, 72H, -(CH₂)₃CH₃).

(8) Wayland, B. B.; Farnos, M. D.; Coffin, V. L. *Inorg. Chem.* **1988**, *27*, 2745.

[®] Abstract published in *Advance ACS Abstracts*, October 15, 1996.

(1) (a) Wayland, B. B.; Sherry, A. E.; Poszmik, G.; Bunn, A. G. *J. Am. Chem. Soc.* **1992**, *114*, 1673. (b) Farnos, M. D.; Woods, B. A.; Wayland, B. B. *J. Am. Chem. Soc.* **1986**, *108*, 3659. (c) Wayland, B. B.; Woods, B. A.; Pierce, R. J. *J. Am. Chem. Soc.* **1982**, *104*, 302. (d) Wayland, B. B.; Duttahmed, A.; Woods, B. A. *J. Chem. Soc., Chem. Commun.* **1983**, 142.

(2) (a) Bunn, A. G.; Wayland, B. B. *J. Am. Chem. Soc.* **1992**, *114*, 6917. (b) Wayland, B. B.; Poszmik, G.; Fryd, M. *Organometallics* **1992**, *11*, 3534. (c) Del Rossi, K. J.; Zhang, X.-X.; Wayland, B. B. *J. Organomet. Chem.* **1995**, *504*, 47. (d) Wayland, B. B.; Del Rossi, K. J. *J. Organomet. Chem.* **1984**, *276*, C27. (e) Del Rossi, K. J.; Wayland, B. B. *J. Am. Chem. Soc.* **1985**, *107*, 7941. (f) Wayland, B. B.; Sherry, A. E.; Coffin, V. L. *J. Chem. Soc., Chem. Commun.* **1989**, 662. (g) Coffin, V. L.; Brennen, W.; Wayland, B. B. *J. Am. Chem. Soc.* **1988**, *110*, 6063. (h) Wayland, B. B.; Woods, B. A.; Coffin, V. L. *Organometallic* **1986**, *5*, 1059.

(3) (a) Zhang, X.-X.; Wayland, B. B. *J. Am. Chem. Soc.* **1994**, *116*, 7897. (b) Wayland, B. B.; Ba, S.; Sherry, A. E. *J. Am. Chem. Soc.* **1991**, *113*, 5305. (c) Sherry, A. E.; Wayland, B. B. *J. Am. Chem. Soc.* **1990**, *112*, 1259.

(4) Bunn, A. G.; Wei, M.; Wayland, B. B. *Organometallics* **1994**, *13*, 3390.

(5) (a) Anderson, D. J.; Eisenberg, R. *Inorg. Chem.* **1994**, *33*, 5379. (b) Anderson, D. J.; Eisenberg, R. *Organometallics* **1996**, *15*, 1697.

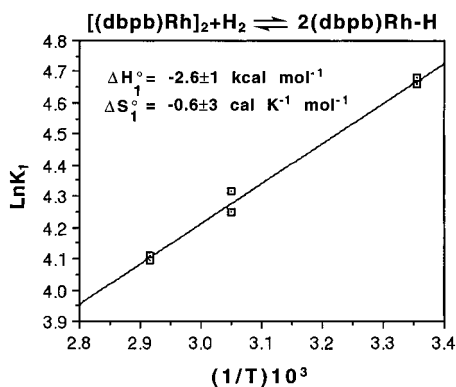
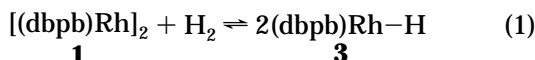


Figure 1. Van't Hoff plot for the reaction of $[(\text{dbpb})\text{Rh}]_2$ with H_2 to form $(\text{dbpb})\text{Rh}-\text{H}$ in THF ($\Delta H^\circ = -2.6 \pm 1.0$ kcal mol $^{-1}$; $\Delta S^\circ = 0.6 \pm 3$ cal K $^{-1}$ mol $^{-1}$).

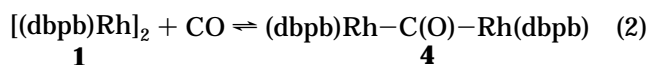
(3) (eq 1). Reaction 1 is slower than the reaction of H_2



with $[(\text{OEP})\text{Rh}]_2$ because the Rh–Rh BDE for **1** is slightly larger and thus **1** is less dissociated into the reactive rhodium(II) monomer. Formation of **3** is conveniently observed by the appearance of a diagnostic high-field doublet in the ^1H NMR (δ –23.6 ppm, $^1J_{\text{Rh}-\text{H}} = 39.0$ Hz).^{9a} Removal of hydrogen results in the re-formation of **1** which demonstrates the well behaved reversibility of reaction 1. Equilibrium constants for reaction 1 in THF were determined by integration of the ^1H NMR intensities for **1**, **3**, and H_2 ($P_{\text{H}_2} = 0.06$ – 0.30 atm) at a series of temperatures (298–333 K) and were used in deriving thermodynamic values for reaction 1 ($\Delta H^\circ_1 = -2.8 \pm 1$ kcal mol $^{-1}$; $\Delta S^\circ_1 = -0.6 \pm 3$ cal K $^{-1}$ mol $^{-1}$) (Figure 1). In contrast with $[(\text{OEP})\text{Rh}]_2$, $[(\text{dbpd})\text{Rh}]_2$ does not give observable hydrocarbon C–H bond reactions which presumably is a thermodynamic consequence of the stronger Rh–Rh bond in **1**.

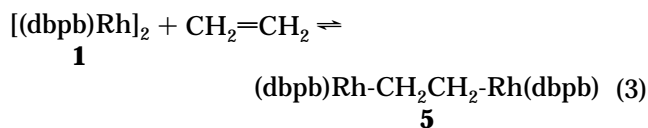
Reaction of **1** with CO ($P_{\text{CO}} = 0.2$ – 0.8 atm) in THF immediately produces a metallo ketone complex, $(\text{dbpb})-$

$\text{Rh}-\text{C}(\text{O})-\text{Rh}(\text{dbpb})^{9b}$ (**4**) (eq 2). The triplet carbonyl



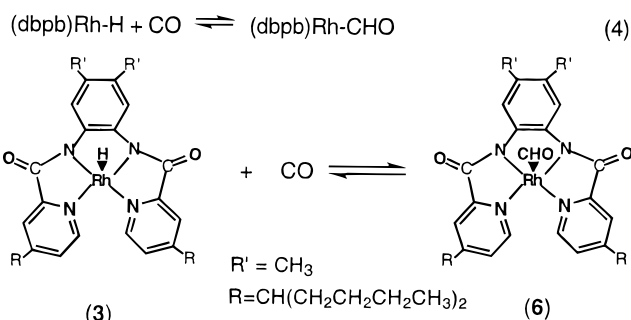
carbon resonance in the ^{13}C NMR of the $^{13}\text{C}(\text{O})$ derivative of **4** ($\delta^{13}\text{C}(\text{O}) = 186.73$ ppm, $^1J_{\text{Rh}-^{13}\text{C}} = 39.5$ Hz) resulting from coupling with two equivalent ^{103}Rh nuclei is particularly diagnostic for the dirhodium ketone complex (**4**).

THF solutions of **1** react with ethene ($P_{\text{C}_2\text{H}_4} = 0.05$ – 0.80 atm, $T = 290$ – 360 K) to produce equilibrium distributions of **1** with an ethylene-bridged complex $(\text{dbpb})\text{Rh}-\text{CH}_2\text{CH}_2-\text{Rh}(\text{dbpb})$ (**5**)^{9c} (eq 3). Reaction 3



is envisioned as occurring by a metalloradical chain mechanism in analogy with that reported by Halpern for the reaction of $[(\text{OEP})\text{Rh}]_2$ with alkenes.¹⁰ The $^{13}\text{C}_2\text{H}_4$ derivative of **5** displays a highly diagnostic AA'XX' pattern in the proton-decoupled ^{13}C NMR ($\delta = 26.47$ ppm, $J_{\text{AA}'} = ^1J_{^{13}\text{C}-^{13}\text{C}} = 33.0$ Hz, $J_{\text{AX}} = ^1J_{^{103}\text{Rh}-^{13}\text{C}} = 28.2$ Hz, $J_{\text{AX}'} = ^2J_{^{103}\text{Rh}-^{13}\text{C}} \sim -1.1$ Hz, $J_{\text{XX}'} = ^3J_{^{103}\text{Rh}-^{103}\text{Rh}} \sim 0.4$ Hz), which demonstrates the presence of a Rh– ^{13}C – ^{13}C –Rh unit. Temperature dependence of the integrated intensity of **1**, **5**, and ethene was used in evaluating the thermodynamic parameters for reaction 3 ($\Delta H^\circ_3 = -12 \pm 1$ kcal mol $^{-1}$; $\Delta S^\circ_3 = -28 \pm 3$ cal mol $^{-1}$ K $^{-1}$, ΔG°_3 (298 K) = -3.7 kcal mol $^{-1}$). Solutions of **1** did not react with propene to an observable extent over the range of conditions where **1** reacts with ethene to form **5**. The bond dissociation enthalpy for a Rh–CH– $(\text{CH}_3)\text{CH}_2-$ fragment is expected to be smaller than a Rh– CH_2CH_2- unit by 6–10 kcal mol $^{-1}$,¹¹ which results in a positive ΔG° (298 K) for the reaction of **1** with propene.

THF solutions of the rhodium hydride complex **3** react with CO ($P_{\text{CO}} = 0.2$ – 0.8 atm) to produce the formyl complex $(\text{dbpb})\text{Rh}-\text{CHO}$ (**6**)^{9d} (eq 4) within the time



required to obtain the ^1H NMR spectrum. A doublet at 11.40 ppm, which splits into a doublet of doublets in the $^{13}\text{C}(\text{O})$ derivative of **6** ($^2J_{\text{Rh}-^{13}\text{C}} = 1.3$ Hz; $^1J_{^{13}\text{C}-\text{H}} = 179$ Hz), is assigned to the formyl hydrogen for **6** (Figure 2). Proton-decoupled ^{13}C NMR for the $^{13}\text{C}(\text{O})$

(10) Paonessa, R. S.; Thomas, N. C.; Halpern, J. *J. Am. Chem. Soc.* **1985**, *107*, 4333.

(11) (a) Wayland, B. B.; Feng, Y.; Ba, S. *Organometallics* **1989**, *8*, 1438. (b) Wayland, B. B. in *Energetics of Organometallic Species*; Simões, M., Ed.; NATO ASI Series C; Kluwer Academic Publishers: Dordrecht, The Netherlands, 1992; Vol. 367, pp 69–74.

(9) (a) ^1H NMR of $(\text{dbpb})\text{Rh}-\text{H}$ (**3**) (THF, δ): 8.69 (d, 2H, py, $^3J = 5.6$ Hz); 8.47 (s, 2H, phenyl); 7.83 (s, 2H, py); 7.31 (d, 2H, py, $^3J = 5.6$ Hz); 2.72 (m, 2H, –CH–); 2.18 (s, 6H, CH_3); 0.8–1.8 (m, 36H, $-(\text{CH}_2)_3\text{CH}_3$); –23.6 (d, 1H, Rh–H, $^1J_{\text{Rh}-\text{H}} = 39.0$ Hz). LR FAB MS (m/e): calc, 700.3; obs, 701. (b) ^1H NMR of $(\text{dbpb})\text{Rh}-\text{C}(\text{O})-\text{Rh}(\text{dbpb})$ (**4**) (THF, δ): 8.45 (s, 4H, phenyl); 8.34 (d, 4H, py, $^3J = 4.9$ Hz); 7.37 (s, 4H, py); 7.24 (d, 4H, py, $^3J = 4.9$ Hz); 2.64 (m, 4H, –CH–); 2.28 (s, 12H, CH_3); 0.8–1.8 (m, 72H, $-(\text{CH}_2)_3\text{CH}_3$). ^{13}C NMR: δ 186.73 (t, 1C, $^1J_{\text{Rh}-^{13}\text{C}} = 39.5$ Hz). (c) ^1H NMR of $(\text{dbpb})\text{Rh}-\text{CH}_2\text{CH}_2\text{Rh}(\text{dbpb})$ (**5**) (THF, δ): 8.47 (d, 4H, py, $^3J = 5.4$ Hz); 8.39 (s, 4H, phenyl); 7.48 (d, 4H, py, $^4J = 1.7$ Hz); 7.08 (d of d, 4H, py, $^3J = 5.4$ Hz, $^4J = 1.7$ Hz); 2.60 (m, 4H, –CH–); 2.17 (s, 12H, CH_3); 0.8–2.0 (m, 72H, $-(\text{CH}_2)_3\text{CH}_3$). ^{13}C NMR (THF): δ 26.47 ppm, $J_{\text{AA}'} = ^1J_{^{13}\text{C}-^{13}\text{C}} = 33.0$ Hz, $J_{\text{AX}} = ^1J_{\text{Rh}-^{13}\text{C}} = 28.2$ Hz, $J_{\text{AX}'} = ^2J_{\text{Rh}-^{13}\text{C}} = -1.1$ Hz, $J_{\text{XX}'} = ^3J_{\text{Rh}-\text{Rh}} = 0.4$ Hz). LR FAB MS (m/e): calc, 1426.6; obs, 1427. (d) ^1H NMR of $(\text{dbpb})\text{Rh}-\text{CHO}$ (**6**) (THF, δ): 11.40 (d of d, Rh– $^{13}\text{C}-\text{H}$, $^1J_{\text{Rh}-\text{H}} = 179$ Hz, $^2J_{\text{Rh}-\text{H}} = 1.3$ Hz); 8.70 (d, 2H, py, $^3J = 5.7$ Hz); 8.51 (s, 2H, phenyl); 7.84 (d, 2H, py, $^4J = 1.7$ Hz); 7.38 (d of d, 2H, py, $^3J = 5.7$ Hz, $^4J = 1.7$ Hz); 2.75 (m, 2H, –CH–); 2.21 (s, 6H, CH_3); 0.8–2.0 (m, 36H, $-(\text{CH}_2)_3\text{CH}_3$). ^{13}C NMR: δ 219.2 (d, Rh– $^{13}\text{C}-\text{CHO}$, $^1J_{\text{Rh}-^{13}\text{C}} = 31.4$ Hz). (e) ^1H NMR of $(\text{Hdbpb})\text{Rh}(\text{CO})_2$ (THF, δ): 10.43 (s, 1H, N–H); 8.44 (d, 1H, py, $^3J = 5.5$ Hz); 8.25 (s, 1H, phenyl); 8.15 (d, 1H, py, $^3J = 5.0$ Hz); 8.05 (d, 1H, py, $^4J = 1.7$ Hz); 8.00 (d, 1H, py, $^4J = 2.0$ Hz); 7.51 (d of d, 1H, py, $^3J = 5.5$ Hz, $^4J = 2.0$ Hz); 7.17 (d of d, 1H, py, $^3J = 5.0$ Hz, $^4J = 1.7$ Hz); 7.02 (s, 1H, phenyl); 2.81 (m, 1H, –CH–); 2.64 (m, 1H, –CH–); 2.28 (s, 3H, CH_3); 2.22 (s, 3H, CH_3); 0.8–2.0 (m, 36H, $-(\text{CH}_2)_3\text{CH}_3$). ^{13}C NMR of the $^{13}\text{C}(\text{O})$ derivative: δ 187.85 (d of d, $^1J_{\text{Rh}-^{13}\text{C}} = 63$ Hz, $^2J_{^{13}\text{C}-^{13}\text{C}} = 8$ Hz); 185.85 (d of d, $^1J_{\text{Rh}-^{13}\text{C}} = 72$ Hz, $^2J_{^{13}\text{C}-^{13}\text{C}} = 8$ Hz). LR FAB MS (m/e): calc, 756.3; obs, 757. (f) ^1H NMR of $(\text{dbpb})\text{Rh}-\text{CH}_2\text{OH}$ (**7**) (THF, δ): 8.60 (d, 2H, py, $^3J = 5.5$ Hz); 8.44 (s, 2H, phenyl); 7.84 (s, 2H, py); 7.29 (d, 2H, py, $^3J = 5.5$ Hz); 5.14 (d of d, 2H, RhCH_2OH , $^2J_{\text{H}-\text{H}} = 7.8$ Hz, $^2J_{\text{Rh}-\text{H}} = 3.2$ Hz); 3.88 (t, 1H, OH, $^2J_{\text{H}-\text{H}} = 7.8$ Hz); 2.71 (m, 2H, –CH–); 2.15 (s, 6H, CH_3); 0.8–1.8 (m, 36H, $-(\text{CH}_2)_3\text{CH}_3$).

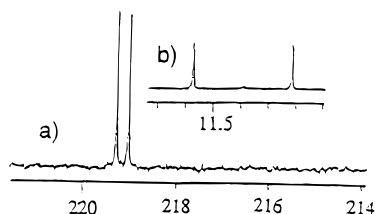


Figure 2. (a) ^1H -decoupled ^{13}C NMR of the formyl unit in $(\text{dbpb})\text{Rh}-^{13}\text{CHO}$ ($\text{THF}-d_8$): $\delta^{13}\text{CHO}$ 219.16 ppm (d, $^1J_{^{103}\text{Rh}-^{13}\text{C}} = 31.4\text{Hz}$). (b) ^1H NMR of the formyl hydrogen ($\text{THF}-d_8$) $\delta^{13}\text{CHO}$ 11.40 ppm ($^1J_{^{13}\text{C}-^1\text{H}} = 179\text{ Hz}$, $^2J_{^{103}\text{Rh}-^1\text{H}} = 1.3\text{ Hz}$).

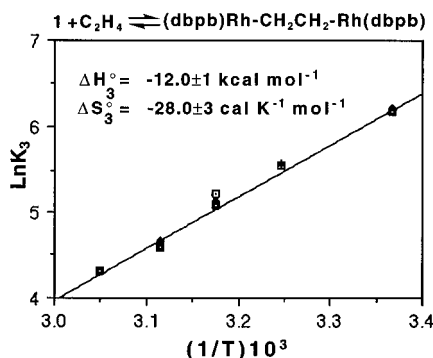
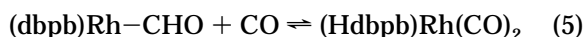


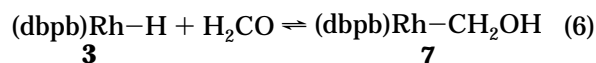
Figure 3. Van't Hoff plot for the reaction of $[(\text{dbpb})\text{Rh}]_2$ with $\text{CH}_2=\text{CH}_2$ to form $(\text{dbpb})\text{Rh}-\text{CH}_2\text{CH}_2-\text{Rh}(\text{dbpb})$ in THF ($\Delta H^\circ = -12 \pm 1\text{ kcal mol}^{-1}$; $\Delta S^\circ = -28 \pm 3\text{ cal K}^{-1}\text{ mol}^{-1}$).

unit exhibits a doublet from ^{103}Rh coupling centered at 219.2 ppm ($^1J_{^{103}\text{Rh}-^{13}\text{C}} = 31.4\text{ Hz}$) (Figure 2). In the presence of CO , the formyl complex **6** slowly disappears over a period of days with the concomitant formation of a rhodium(I) dicarbonyl complex $(\text{Hdbpb})\text{Rh}^{\text{I}}(\text{CO})_2^{9\text{e}}$ as the final thermodynamic product (eq 5).

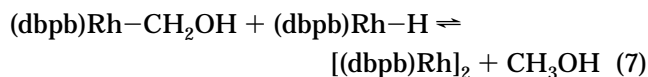


The hydride, $(\text{dbpb})\text{Rh}-\text{H}$, also reacts rapidly with H_2CO to form the hydroxymethyl complex, $^{9\text{f}}$ $(\text{dbpb})\text{Rh}-$

CH_2OH (**7**) (eq 6). The hydroxymethyl complex (**7**) is



observed to react with solutions of $(\text{dbpb})\text{Rh}-\text{H}/\text{H}_2$ (353 K) to form methanol and $[(\text{dbpb})\text{Rh}]_2$ (eq 7). Relatively



fast reactions of $(\text{dbpd})\text{Rh}-\text{H}$ with CO and H_2CO compared to the reactions of (porphyrin) $\text{Rh}-\text{H}$ suggest that the more flexible nonmacrocyclic ligand may permit a reaction pathway not available to rigid porphyrin macrocyclic complexes.

Reactions of $(\text{dbpb})\text{Rh}-\text{H}$ with CO and H_2CO that produce rhodium formyl and hydroxymethyl derivatives with improved kinetics compared with (porphyrin) $\text{Rh}-\text{H}$ reactions and intermolecular reductive elimination of CH_3OH illustrate patterns of reactivity relevant to homogenous hydrogenation of carbon monoxide. 12 Thermodynamic instability of the formyl complex in the presence of CO with respect to a rhodium(I) dicarbonyl is a property also manifested by the rhodium salen derivatives, 4,5 and this feature currently limits application of flexible nonmacrocyclic ligand complexes as catalysts for CO reduction and hydrogenation.

Acknowledgment. Support for this research by the Department of Energy, Division of Chemical Sciences, Office of Basic Energy Sciences, Grant DE-FG02-86ER 13615, is gratefully acknowledged.

OM960492H

(12) (a) Dombek, B. D.; *Adv. Catal.* **1983**, *32*, 325. (b) Rathke, J. W.; Feder, H. M. *J. Am. Chem. Soc.* **1978**, *100*, 3623. (c) Fahey, D. R. *J. Am. Chem. Soc.* **1981**, *103*, 136. (d) Costa, L. C. *Catal. Rev. Sci. Eng.* **1983**, *25*, 325.